

Spin and charge ordering in the dimerized Hubbard model

S. Caprara

Dipartimento di Fisica, Università di Roma "La Sapienza" and Istituto Nazionale per la Fisica della Materia, Unità di Roma 1, Piazzale Aldo Moro 2, 00185 Roma, Italy

M. Avignon

LEPES - CNRS, Boîte Postale 166, 38042 Grenoble Cedex 9, France

O. Navarro

Instituto de Investigaciones en Materiales, UNAM, Apartado Postal 70-360, 04510, México Distrito Federal, Mexico

(Received 17 February 1999)

We study the effect of a chemically or deformation-induced charge-density wave on the spin-density-wave ground state of the Hubbard model at half-filling. We also consider the effect of a lattice deformation associated with a dimerization of the hopping term, thus introducing a competition with a paramagnetic bond-alternating phase. The slave-boson approach is used as an interpolation scheme to treat the electronic correlations from weak to strong coupling and determine the phase diagram of the model. We also apply our results to describe the neutral-ionic transition in organic mixed-stack donor-acceptor crystals.

I. INTRODUCTION

In the absence of a direct electron-electron mechanism for the onset of a charge-density wave (CDW), an induced charge transfer between neighboring sites may be produced by a modulation of the chemical environment, which results in the so-called chemical dimerization of the system. Such is, for instance, the case of the π -bond chains on the reconstructed (111) surfaces of C and Si.¹ Other examples of chemically induced charge transfer are found in organic mixed-stack donor-acceptor crystals, which are often found either in the quasi neutral or in the fully ionized configuration, as a consequence of the competition between covalency and ionic effects.² When the coupling of the electronic density to the lattice is taken into account, the charge transfer may be accompanied (or produced) by a deformation of the lattice.

The issue we want to address in this paper is the effect of such kinds of chemical and/or lattice dimerization in nesting-type models for spin-density-wave (SDW) antiferromagnets, such as the Hubbard model with nearest-neighbor hopping at half-filling. The SDW in the Néel-like antiferromagnetic (AFM) phase and the CDW associated with the structure of the chemical and/or lattice dimerization that we are going to analyze in the following are characterized by the same commensurate wave vector, so that the competition between charge and spin ordering is essentially due to the way in which different mechanisms affect the gap in the excitation spectrum, in the charge and spin channel.

Two scenarios are possible: either the existence of a spin-ordered state excludes any charge ordering and vice versa, or charge and spin order coexist, possibly with a mutual reduction.

Indeed when the charge transfer between neighboring sites is induced by an external potential (e.g., a modulation of the chemical environment), a coexistence is possible if the (intra-atomic) energy scale responsible for antiferromagnetic

order is sufficiently large.³ On the other hand, when the charge modulation is produced by the coupling of electron density to an elastic lattice deformation, the presence of spin order excludes charge ordering by suppressing anharmonic effects in the self-consistent elastic potential. In such a case the SDW phase stays undeformed, whereas the deformed CDW phase is paramagnetic (PM).⁴

It must be pointed out that other lattice deformations, not directly related to a modulation of the electron density, may compete with antiferromagnetism in nesting-type systems. For instance, when the lattice dimerizes, with the formation of long and short bonds, the overlap integral between neighboring sites is modulated, and a gap opens at the boundary of the Brillouin zone thus stabilizing the PM phase with respect to the SDW phase when the coupling to the lattice deformation is strong enough to compete with the (intra-atomic) energy scale responsible for spin ordering.³

When some or all of the above mechanisms are present, different physical behaviors are possible. Without attempting to provide a full variety of phase diagrams, which would necessarily refer to specific physical systems, in this paper we emphasize generic features of the structures which may arise in dimerized systems due to the interplay of competitive mechanisms leading to different ordered phases.

The scheme of the paper is as follows. In Sec. II we introduce an extended Hubbard model and discuss the physical meaning of the different terms appearing in our model Hamiltonian. In Sec. III we discuss the mean-field phases which may arise due to the interplay between charge and spin degrees of freedom. In particular, Sec. III A is devoted to the effect of a chemical dimerization on the SDW ground state of the Hubbard model and Sec. III B deals with the effect of a bond dimerization. In Sec. III C we discuss the effects of the coupling of electron density to an elastic lattice deformation. In Sec. III D we show that the dimerized Hubbard model introduced in Sec. II may be used, in a suitable limit, to discuss the neutral-ionic transition occurring in

some organic mixed-stack donor-acceptor crystals. Concluding remarks are found in Sec. IV.

II. THE MODEL

For the sake of definiteness, the physical scenario discussed in the preceding section is analyzed in this paper by means of the one-dimensional extended Hubbard model defined by the Hamiltonian

$$\begin{aligned} \tilde{\mathcal{H}} = & -t \sum_{l,\sigma} (\tilde{f}_{l,\sigma}^+ \tilde{f}_{l+1,\sigma} + \text{H.c.}) + I \sum_{l,\sigma} (-1)^l \tilde{f}_{l,\sigma}^+ \tilde{f}_{l,\sigma} \\ & + U \sum_l \tilde{f}_{l,\uparrow}^+ \tilde{f}_{l,\uparrow} \tilde{f}_{l,\downarrow}^+ \tilde{f}_{l,\downarrow} - g_t \sum_{l,\sigma} y_{l,l+1} (\tilde{f}_{l,\sigma}^+ \tilde{f}_{l+1,\sigma} + \text{H.c.}) \\ & + g_a \sum_{l,\sigma} x_l \left(\tilde{f}_{l,\sigma}^+ \tilde{f}_{l,\sigma} - \frac{n}{2} \right) + \frac{K_t}{2} \sum_l y_{l,l+1}^2 + \frac{K_a}{2} \sum_l x_l^2, \end{aligned} \quad (1)$$

where $l = 1, \dots, N_s$ labels the sites of the chain, the intersite distance is taken $a = 1$, the fermion operators $\tilde{f}_{l,\sigma}^+, \tilde{f}_{l,\sigma}$ act in the Wannier representation, t is the nearest-neighbor hopping parameter, I is the amplitude of a staggered local potential, which is produced by some external (crystal) field associated, for instance, with the modulation of the chemical environment, and U is the on-site Coulombic repulsion. The electrons are coupled to the lattice and we consider two possible terms. The constant $g_t \approx \partial t / \partial y$ couples the electrons to a bond deformation $y_{l,l+1}$, with elastic constant K_t , which induces a change in the hopping parameter, whereas $g_a \approx \partial E_a / \partial x$ couples electron density fluctuations with respect to the average value $n/2$ (per spin) to a lattice deformation x_l , with elastic constant K_a , which induces a change in the atomic energy E_a . We have chosen the reference energy in Eq. (1) such that $E_a = 0$.

This is the simplest model to investigate the conditions for the coexistence of a SDW, which is promoted by the U term, and a CDW, produced by the I term and/or the coupling of electron density fluctuations to the local deformation x_l . The possibility for a dimerization of the hopping term due to the coupling of electrons to a bond deformation $y_{l,l+1}$ is also taken into account as an alternative mechanism which competes with AFM spin ordering in dimerized systems. It must be observed that in Eq. (1) we are considering two different lattice deformations coupled to the electron density fluctuations and to the hopping term, respectively. However, we are not going, in the following, to consider the interplay of the two electron-lattice terms, i.e., we shall discuss the effect of a deformation which modifies either the local potential or the overlap of the electron wave functions on neighboring sites. In real systems the two effects might be associated with a single lattice deformation (e.g., a bond deformation which induces a modulation in both the hopping term and the atomic term) or with two independent lattice modes (a change in the atomic term might be produced by a deformation which does not change the bond length). In such a case a deeper analysis of the different modes of the lattice is required to describe the interplay of different distortions

and the resulting physical scenarios in each specific physical system. Such a detailed analysis is beyond the scope of our paper.

Finally we note that, as far as the properties of the electronic spectrum are concerned, the parametrization of the electron-lattice coupling through the constants g_t, K_t and g_a, K_a is redundant. In the following we adopt a standard notation and introduce the dimensionless deformation $Y_{l,l+1} = g_t y_{l,l+1} / t$, the dimensionless coupling constant $\lambda = 2g_t^2 / \pi K_t t$, and the parameters $X_l = g_a x_l$ and $E_p = g_a^2 / 2K_a$, both with the dimensions of an energy. The electron-lattice Hamiltonian then reads

$$\begin{aligned} & -t \sum_{l,\sigma} Y_{l,l+1} (\tilde{f}_{l,\sigma}^+ \tilde{f}_{l+1,\sigma} + \text{H.c.}) + \sum_{l,\sigma} X_l \left(\tilde{f}_{l,\sigma}^+ \tilde{f}_{l,\sigma} - \frac{n}{2} \right) \\ & + \frac{t}{\pi \lambda} \sum_l Y_{l,l+1}^2 + \frac{1}{4E_p} \sum_l X_l^2, \end{aligned} \quad (2)$$

from which it is evident that the two parameters λ, E_p completely determine the properties of the electronic spectrum in the deformed state, while the coupling constants g_t, g_a determine only the properties of the deformed lattice, i.e., the self-consistent values of the deformations $y_{l,l+1}, x_l$.

We emphasize that, in the zero-temperature limit considered in this paper, due to the mean-field character of our results, the choice of a one-dimensional model is essentially adopted to simplify the forthcoming analytical and numerical calculations, and does not imply by itself any severe limitation to their validity. One should, for instance, keep in mind that in real quasi-one-dimensional systems the chains are (loosely) bound with one another and the corresponding characteristic energy scale t_\perp determines the crossover to a genuine one-dimensional behavior at some finite temperature. On the other hand, mean-field results are not modified as long as, for instance, $t_\perp \ll t$.

III. MEAN-FIELD RESULTS

This section is devoted to the analysis of the different ordered structures that may appear due to the interplay of charge and spin degrees of freedom and to the relative relevance of the different terms appearing in Eq. (1).

A. Chemical dimerization

Let us first consider the case in which the coupling of electrons to the lattice is neglected (i.e., $g_t, g_a = 0$).⁵ In the noninteracting ($U = 0$) half-filled ($n = 1$) system, a charge modulation is induced by the external field I . If we let n_A and n_B be the number of particles on the two inequivalent sites of the bi-partite chain, with even and odd site index l , respectively ($n_A + n_B = 2$ in the half-filled case), then the CDW amplitude $m_e \equiv \frac{1}{2}(n_B - n_A)$ is given by

$$m_e = \frac{I}{\pi} \int_{-\pi/2}^{\pi/2} \frac{dk}{\sqrt{I^2 + 4t^2 \cos^2 k}}, \quad (3)$$

which saturates towards 1 as I is increased. Here we point out that, due to the logarithmic divergence of the integral in Eq. (3) as $I \rightarrow 0$, the curve $m_e(I)$ starts with an infinite slope close to $I = 0$. This behavior is a consequence of the perfect

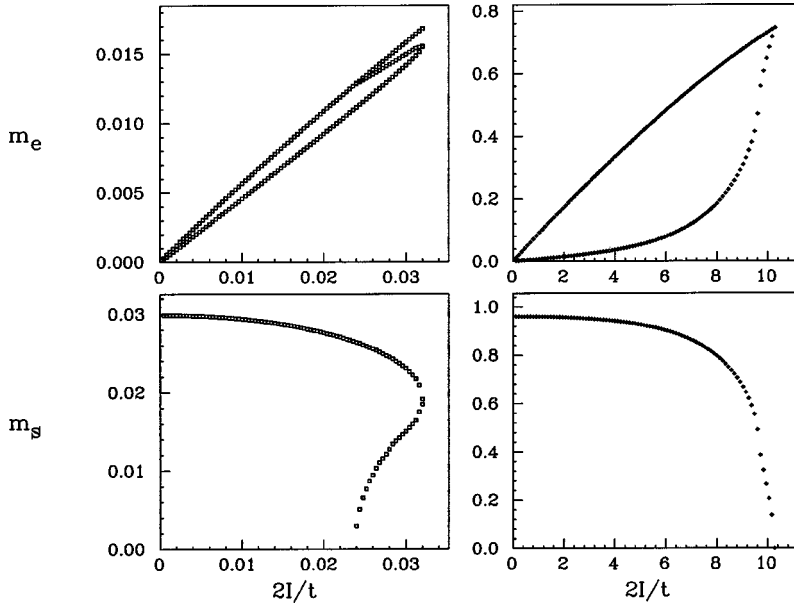


FIG. 1. Charge- (top) and spin- (bottom) density-wave amplitudes within the HF approximation as a function of $2I/t$, for $U/t=1$ (left) and $U/t=10$ (right).

nesting of the Fermi surface with respect to the characteristic wave vector of the external potential discussed in this paper.

On the other hand, when $I=0$, the possibility for an AFM state arises as soon as $U>0$, again due to the perfect nesting of the Fermi surface at half-filling. This state can be characterized by a SDW amplitude $m_s \equiv n_{A\uparrow} - n_{A\downarrow} = n_{B\downarrow} - n_{B\uparrow}$. At $I=0$, m_s is an increasing function of the ratio U/t , both in the Hartree-Fock and slave-boson approximations.⁶ As $U/t \rightarrow \infty$, m_s saturates towards 1.

The simultaneous presence of the staggered external field I and of the on-site electron-electron interaction U implies an interplay of charge and spin degrees of freedom which we want to clarify in the following. Before turning to the slave-boson (SB) technique, we shall briefly analyze the competition of spin and charge ordering within the Hartree-Fock (HF) approximation, which applies in the weak-coupling limit $U/t \ll 1$, to provide, as a starting point, a clearer insight into the physics of the dimerized Hubbard model.

On a general ground, indeed, the field I opens a gap in the charge channel, thus unfavoring SDW formation, whereas the interaction U opens a gap in the spin channel and can substantially reduce the CDW amplitude even in the presence of a sizeable external field I . However, self-consistency imposes a complicate interdependence of m_s and m_e , which can give rise to discontinuous (first-order) phase transitions between magnetic and nonmagnetic phases.

In the following we make use of the parametrization $n_{A\sigma} = \frac{1}{2}(1 + \sigma m_s - m_e)$, $n_{B\sigma} = \frac{1}{2}(1 - \sigma m_s + m_e)$, for the average number of electrons of a given spin σ on a site of the A or B sublattice, respectively. The HF spin-dependent atomic levels are then given by $E_{A\sigma} \equiv I + U n_{A,-\sigma} = I + U(1 - \sigma m_s - m_e)/2$ and $E_{B\sigma} \equiv -I + U n_{B,-\sigma} = -I + U(1 + \sigma m_s + m_e)/2$ so that the gap in the energy spectrum for electrons of spin σ is given by $\Delta_\sigma \equiv \frac{1}{2}(E_{A\sigma} - E_{B\sigma}) = I - U(m_e + \sigma m_s)/2$. This expression for the energy gap gives an insight into the competition between external potential and on-site Coulombic repulsion, with respect to charge and spin order. Indeed, the repulsive U term tends to reduce the gap in the charge channel, but affects the two spin channels with

different signs, thus stabilizing the spin-ordered phase even in the presence of a charge modulation.

The self-consistency equations for m_s and m_e are then³

$$m_s = \frac{1}{2\pi t} \sum_{\sigma} (-\sigma) \kappa_{\sigma} \Delta_{\sigma} \mathcal{K}(\kappa_{\sigma}^2), \quad (4)$$

$$m_e = \frac{1}{2\pi t} \sum_{\sigma} \kappa_{\sigma} \Delta_{\sigma} \mathcal{K}(\kappa_{\sigma}^2),$$

where $\kappa_{\sigma} = 2t/\sqrt{4t^2 + \Delta_{\sigma}^2}$ and $\mathcal{K}(x)$ is the complete elliptic integral of the first kind. Observe that the two equations in Eq. (4) differ in the relative sign of the two terms appearing in the sum over σ in the right-hand side. The HF approximation thus implies that a phase with zero staggered magnetization will have a larger CDW amplitude than a phase with coexisting CDW and SDW.

Introducing the two auxiliary parameters $m_{\sigma} = m_e + \sigma m_s$, so that $\Delta_{\sigma} = I - U m_{\sigma}/2$, one can reduce the above equations (4) to $m_{\uparrow} = (1/\pi t) \kappa_{\downarrow} \Delta_{\downarrow} \mathcal{K}(\kappa_{\downarrow}^2)$ and $m_{\downarrow} = (1/\pi t) \kappa_{\uparrow} \Delta_{\uparrow} \mathcal{K}(\kappa_{\uparrow}^2)$, from which it is evident that m_{\uparrow} is determined via m_{\downarrow} and vice versa. From a numerical point of view, the last two equations can thus be reduced to an equation for a single variable (for instance m_{\uparrow}), the other being immediately determined once the first is known.

The energy per lattice site corresponding to each self-consistent solution of Eq. (4) is

$$E = -\frac{U}{4} m_{\uparrow} m_{\downarrow} - \frac{2t}{\pi} \sum_{\sigma} \frac{\mathcal{E}(\kappa_{\sigma}^2)}{\kappa_{\sigma}},$$

where $\mathcal{E}(x)$ is the complete elliptic integral of the second kind.

We investigated the numerical solution of the self-consistency equations (4) and found that the paramagnetic-antiferromagnetic transition predicted by the HF approximation is of first order in the weak-coupling regime, but becomes of second order in the strong-coupling regime (see Fig. 1).

However, when $U > t$ the HF predictions are unreliable and the SB approach⁷ is more appropriate to deal with the intermediate- to strong-coupling limit $U/t > 1$. Moreover, since the SB formalism provides a description which agrees with HF results in the weak-coupling regime, to avoid switching between two different notations, in the rest of the paper we shall apply the SB approach as an interpolation scheme down to $U/t = 0$.

To describe a bi-partite lattice, we introduce a set of Kotliar-Ruckenstein SB operators,⁸ with the corresponding Lagrange multipliers, on each sublattice. At the mean-field level, in the case of coexisting CDW and SDW, we introduce the parametrization

$$\begin{aligned} \langle p_{l,\sigma} \rangle &= p_{A\sigma} & \langle p_{l,\sigma} \rangle &= p_{B\sigma} \\ \langle e_l \rangle &= e_A & \langle e_l \rangle &= e_B \\ \langle d_l \rangle &= d_A \quad \text{for } l \in A; & \langle d_l \rangle &= d_B \quad \text{for } l \in B, \\ \langle \lambda_l \rangle &= \lambda_A & \langle \lambda_l \rangle &= \lambda_B \\ \langle \Lambda_{l,\sigma} \rangle &= \Lambda_{A\sigma} & \langle \Lambda_{l,\sigma} \rangle &= \Lambda_{B\sigma} \end{aligned} \quad (5)$$

where, as in the previous sections, A and B indicate the two different sublattices, $p_{l,\sigma}, e_l, d_l$ are the SB operators to label singly occupied, empty, and doubly occupied sites, respec-

tively, λ_l , is the Lagrange multiplier to enforce the completeness relation on each site l , and $\Lambda_{l,\sigma}$ ($\sigma = \uparrow, \downarrow$) are the Lagrange multipliers to enforce correct fermion counting. To connect the above parameters to the parameters introduced in the HF approximation, observe that it is possible to define $p_{A(B)\sigma} \equiv p_0 + (-)\sigma m_s/4p_0$, $d_{A(B)} \equiv d_0 - (+)m_e/4d_0$, $e_{A(B)} \equiv d_0 + (-)m_e/4d_0$, and $\Lambda_{A(B)\sigma} \equiv U/2 - (+)[\Lambda_c + \sigma\Lambda_s]$, where m_s, m_e are the SDW and CDW amplitudes as in the preceding section, and p_0, d_0 and Λ_c, Λ_s are new parameters, the last two playing the role of the charge and spin effective fields, respectively, even though, in the SB approximation, $\Lambda_c \neq Um_e/2$ and $\Lambda_s \neq Um_s/2$. We point out that the above connection reduces the number of free parameters. Nonetheless, we did not eliminate this redundancy while numerically solving the self-consistency equations (see below), so that all the parameters introduced in Eq. (5) were allowed to vary independently. Once self-consistency was achieved, we checked that all self-consistent solutions could be reexpressed in terms of the fewer parameters introduced above.

The average particle density per spin on each sublattice is given by $n_{A\sigma} \equiv \langle f_{l,\sigma}^+ f_{l,\sigma} \rangle = d_A^2 + p_{A\sigma}^2$ for $i \in A$ and $n_{B\sigma} \equiv \langle f_{l,\sigma}^+ f_{l,\sigma} \rangle = d_B^2 + p_{B\sigma}^2$ for $i \in B$, where $f_{l,\sigma}$ are the pseudofermion operators in the Wannier representation. After introducing the effective hopping parameter $\tilde{t}_\sigma = t z_\sigma^2$, where

$$z_\sigma^2 \equiv z_{A\sigma} z_{B\sigma} = \frac{(p_{A\sigma} e_A + d_{A\sigma}) (p_{B\sigma} e_B + d_{B\sigma})}{\sqrt{(1 - e_A^2 - p_{A\sigma}^2)(1 - d_A^2 - p_{A\sigma}^2)(1 - e_B^2 - p_{B\sigma}^2)(1 - d_B^2 - p_{B\sigma}^2)}}$$

is the hopping renormalization factor, we performed a Fourier transform in the reduced-Brillouin-zone scheme to obtain the mean-field Hamiltonian in the form

$$\begin{aligned} \mathcal{H}_{mf} &= \sum_{k,\sigma} (f_{k,\sigma}^+ f_{k+Q,\sigma}^+) \begin{pmatrix} E_\sigma - 2\tilde{t}_\sigma \cos k & \Delta_\sigma \\ \Delta_\sigma & E_\sigma + 2\tilde{t}_\sigma \cos k \end{pmatrix} \\ &\times \begin{pmatrix} f_{k,\sigma} \\ f_{k+Q,\sigma} \end{pmatrix} + \frac{N_s U}{2} (d_A^2 + d_B^2) \\ &- \frac{N_s}{2} \sum_\sigma [\Lambda_{A\sigma} (p_{A\sigma}^2 + d_A^2) + \Lambda_{B\sigma} (p_{B\sigma}^2 + d_B^2)] \\ &+ \frac{N_s}{2} \left[\lambda_A \left(\sum_\sigma p_{A\sigma}^2 + e_A^2 + d_A^2 - 1 \right) \right. \\ &\left. + \lambda_B \left(\sum_\sigma p_{B\sigma}^2 + e_B^2 + d_B^2 - 1 \right) \right]. \end{aligned} \quad (6)$$

In the above formulas $f_{k,\sigma}^+, f_{k,\sigma}$ are the pseudofermion operators in the Block representation, the sum over k runs over the reduced Brillouin zone (i.e., $k \in [-\pi/2, \pi/2]$), Q is the wave vector of both the commensurate SDW structure and the external potential, equal to one-half of the reciprocal-lattice vector of the undimerized lattice, $E_\sigma = \frac{1}{2}(\Lambda_{A\sigma} + \Lambda_{B\sigma}) = U/2$ is actually independent of σ , $\Delta_\sigma = \frac{1}{2}(2I + \Lambda_{A\sigma} - \Lambda_{B\sigma}) = I - (\Lambda_c + \sigma\Lambda_s)$, and N_s is the number of lat-

tice sites. The eigenvalues of the matrix Hamiltonian in Eq. (6) give the quasiparticle bands $E_{k\sigma}^\pm = U/2 \pm \sqrt{\Delta_\sigma^2 + 4\tilde{t}_\sigma^2 \cos^2 k}$. At half-filling and zero temperature only the two lower (valence) bands are occupied and the mean-field energy per lattice site is

$$E = E_0 + \frac{1}{N_s} \sum_{k,\sigma} E_{k\sigma}^-, \quad (7)$$

where E_0 is the energy per lattice site associated with the last two lines in Eq. (6). The self-consistency equations are obtained by requiring the mean-field energy, Eq. (7), to be stationary with respect to the parameters in Eq. (5), and have the general form⁹

$$\frac{\partial E_0}{\partial P_\alpha} + \frac{1}{N_s} \sum_{k,\sigma} \frac{\partial E_{k\sigma}^-}{\partial P_\alpha} = 0, \quad (8)$$

where P_α represents generically one of the parameters in Eq. (5).

We found that, contrary to the HF approximation, the SB approximation gives a first-order antiferromagnetic-paramagnetic phase transition even in the strong-coupling regime ($U \gg t$). The region of hysteresis is generally narrow when $U \gg t$, and the jump of the SDW amplitude at the transition is sizeable (see Fig. 2). This means that, at large U/t , the AFM phase is the only stable phase in a wide range of

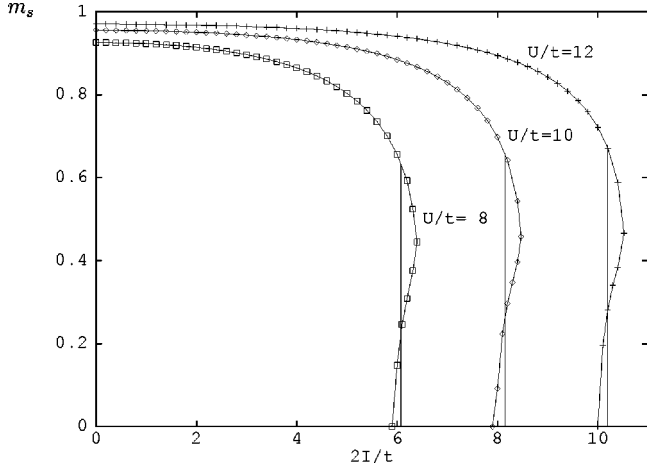


FIG. 2. Spin-density-wave amplitude within the SB approximation as a function of $2I/t$, for $U/t=8,10,12$. The vertical lines in the coexistence regions locate the first-order AFM-PM phase-transition points and represent the corresponding jump in the SDW amplitude.

values of the external field I , but is rapidly suppressed once the competition with a metastable PM phase sets in. The PM state is always characterized by a larger CDW amplitude at the transition point (see Fig. 3). The corresponding phase diagram is found in the $2I/t$ vs U/t plane in Fig. 5.

B. Bond dimerization

In this section we discuss the effect of a dimerization of the hopping term in Eq. (1) due to the coupling of electrons to a bond deformation $y_{l,l+1}$, by assuming a finite g_t . According to our initial assumptions, we consider here only the case $g_a=0$. We shall describe the electronic properties of the model in terms of the dimensionless deformation $Y \equiv Y_{AB} = -Y_{BA}$ and of the dimensionless coupling constant λ appearing in Eq. (2). The mean-field Hamiltonian now reads

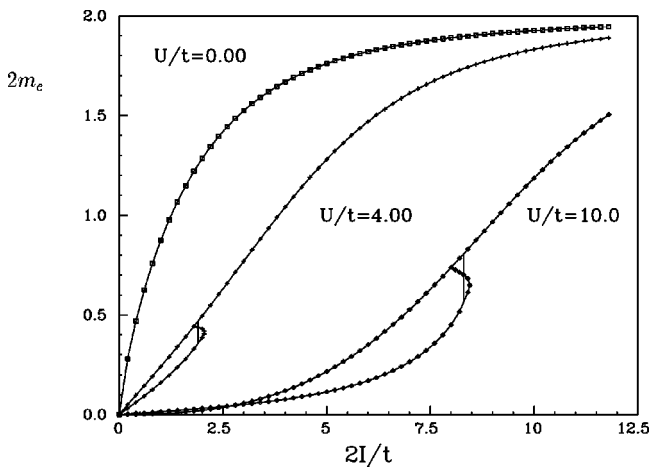


FIG. 3. Charge-density-wave amplitude within the SB approximation as a function of $2I/t$, for the representative values $U/t=0.0, 4.0, 10.0$. The vertical lines in the coexistence regions locate the first-order AFM-PM phase-transition points and represent the corresponding jumps in the CDW amplitude.

$$\begin{aligned} \mathcal{H}_{mf} = & \sum_{k,\sigma} (f_{k,\sigma}^+ f_{k+Q,\sigma}^+) \\ & \times \begin{pmatrix} E_\sigma - 2\tilde{t}_\sigma \cos k & \Delta_\sigma - 2i\tilde{t}_\sigma Y \sin k \\ \Delta_\sigma + 2i\tilde{t}_\sigma Y \sin k & E_\sigma + 2\tilde{t}_\sigma \cos k \end{pmatrix} \begin{pmatrix} f_{k,\sigma} \\ f_{k+Q,\sigma} \end{pmatrix} \\ & + \frac{N_s U}{2} (d_A^2 + d_B^2) - \frac{N_s}{2} \sum_\sigma [\Lambda_{A\sigma} (p_{A\sigma}^2 + d_A^2) \\ & + \Lambda_{B\sigma} (p_{B\sigma}^2 + d_B^2)] + \frac{N_s}{2} \left[\lambda_A \left(\sum_\sigma p_{A\sigma}^2 + e_A^2 + d_A^2 - 1 \right) \right. \\ & \left. + \lambda_B \left(\sum_\sigma p_{B\sigma}^2 + e_B^2 + d_B^2 - 1 \right) \right] + \frac{N_s t}{\pi \lambda} Y^2. \end{aligned} \quad (9)$$

The eigenvalues of the matrix Hamiltonian in Eq. (9) give the quasiparticle bands, which after some simple manipulations may be cast in the form $E_{k\sigma}^\pm = U/2 \pm \sqrt{\bar{\Delta}_\sigma^2 + 4\tilde{t}_\sigma^2 \cos^2 k}$, where $\bar{\Delta}_\sigma \equiv \sqrt{\Delta_\sigma^2 + 4\tilde{t}_\sigma^2 Y^2}$ is the effective gap for electrons of spin σ , increased by the effect of the bond dimerization, and $\tilde{t}_\sigma \equiv \sqrt{t_\sigma^2 (1 - Y^2)}$ is the effective bandwidth for electrons of spin σ , reduced by the bond dimerization. We point out that, although the resulting spectrum is real for all $|Y|$, as an obvious consequence of the hermiticity of the matrix Hamiltonian in Eq. (9), it preserves the same structure as the spectrum at $Y=0$ only as long as \tilde{t}_σ is real, i.e., $|Y| \leq 1$. Thus, in the following, we limit our analysis to values of the electron-lattice coupling constant λ such that $Y^2 \leq 1$.

When $I=0$, $U>0$, a PM phase is stabilized with respect to the SDW phase in the region of small U/t by the opening of a gap at the boundary of the Brillouin zone. The SDW phase is always undeformed (i.e., spin ordering and bond deformation do not coexist) and at sufficiently large U/t it has a lower energy than the PM dimerized phase. A first-order phase transition between a PM phase and a SDW antiferromagnetic phase is then produced, for instance, by increasing U/t at a fixed λ . The value of U/t at the phase transition increases with increasing λ . To be consistent with the requirement that $Y^2 \leq 1$, we followed the transition line up to $\lambda=0.5$ (see the U/t vs λ plane in Fig. 5).

On the other hand, if $U=0$ and $I>0$, there are two possibilities: if I is small, the resulting CDW phase has dimerized bonds, i.e., $Y \neq 0$. As I is increased, the CDW phase with dimerized bonds undergoes a second-order phase transition towards a CDW phase with undimerized bonds, where $Y=0$ (see Fig. 4 and the $2I/t$ vs λ plane in Fig. 5).

When $U, I, \lambda > 0$, the phase diagram is divided into three regions. For large U/t , a SDW is present and coexists with a CDW as soon as $I>0$. The bonds in the spin-ordered phase are never dimerized ($Y=0$). For large I/t , the pure CDW phase exists, and the bonds are not dimerized. Finally, for small I/t and U/t a PM phase exists, which is characterized by dimerized bonds when $\lambda > 0$, and a finite CDW amplitude as soon as $I>0$. The transition between the CDW phases with dimerized and undimerized bonds is of second order. The SDW phase may either undergo a direct phase transition to the CDW phase with undimerized bonds, or to the CDW phase with dimerized bonds, which in turn evolves continu-

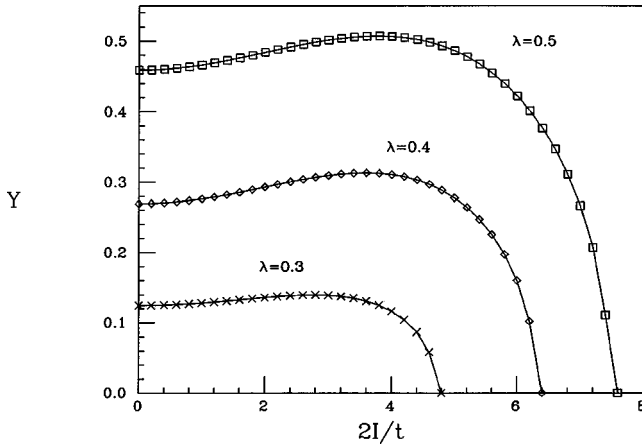


FIG. 4. Mean-field value of the bond dimerization Y within the SB approximation as a function of $2I/t$ for the representative value $U/t=6$ and different values of the dimensionless electron-lattice coupling constant λ . It must be observed that the curves are purely indicative of a generic behavior. At $U/t=6$, indeed, the PM phase is a local minimum of the energy, but the SDW AFM phase has a lower energy (see Fig. 5).

ously towards the CDW with undimerized bonds, as I/t is increased. It is interesting to observe that, at sufficiently large U/t , the bond dimerization Y in the CDW phase is first increasing with increasing I/t , reaches a maximum, and then decreases until it vanishes at the phase transition to the CDW phase with undimerized bonds (see Fig. 4). [Observe that this figure refers to a region of the parameter space where the PM phase is a local (metastable) minimum, and the AFM phase has a lower energy. It is, however, indicative of a generic behavior.³] A schematic idea of the full phase diagram is given in Fig. 5.

We point out again that our analysis was limited to the values of λ such that $Y^2 \ll 1$ and to values of U/t not too close to the Brinkman-Rice transition point in the PM phase,^{8,10} at which the effective (i.e., renormalized by slave bosons) hopping amplitude vanishes, so that the coupling of electrons to the deformation $y_{l,l+1}$ loses its meaning within our approach.

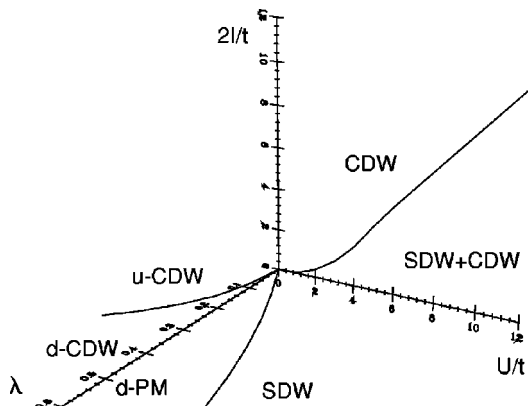


FIG. 5. Schematic phase diagram of the Hubbard model in the presence of chemical and bond dimerization, within the SB approximation. The prefix d- (u-) stand for dimerized (undimerized) bonds.

C. Lattice dimerization

In this section we briefly describe the properties of the Hubbard model in the presence of a coupling of the electron density fluctuations to the lattice, through a coupling constant g_a . According to the general scheme of our paper, we consider here only the case $g_t=0$. The electronic properties of the model will be discussed in terms of the change in the atomic energy $X \equiv X_A = -X_B$ associated with a lattice dimerization, and of the effective coupling constant E_p (both with the dimensions of an energy) appearing in Eq. (2). We shall also introduce the dimensionless parameter $\varepsilon_p \equiv E_p/t$, which provides a measure of the deformation energy in the atomic limit ($\sim E_p$) with respect to the kinetic energy of the free electrons ($\sim t$). The mean-field Hamiltonian is then

$$\begin{aligned} \mathcal{H}_{mf} = & \sum_{k,\sigma} (f_{k,\sigma}^+ f_{k+Q,\sigma}^+) \begin{pmatrix} E_\sigma - 2\tilde{t}_\sigma \cos k & \Delta_\sigma + X \\ \Delta_\sigma + X & E_\sigma + 2\tilde{t}_\sigma \cos k \end{pmatrix} \\ & \times \begin{pmatrix} f_{k,\sigma} \\ f_{k+Q,\sigma} \end{pmatrix} + \frac{N_s U}{2} (d_A^2 + d_B^2) \\ & - \frac{N_s}{2} \sum_\sigma [\Lambda_{A\sigma} (p_{A\sigma}^2 + d_A^2) + \Lambda_{B\sigma} (p_{B\sigma}^2 + d_B^2)] \\ & + \frac{N_s}{2} \left[\lambda_A \left(\sum_\sigma p_{A\sigma}^2 + e_A^2 + d_A^2 - 1 \right) \right. \\ & \left. + \lambda_B \left(\sum_\sigma p_{B\sigma}^2 + e_B^2 + d_B^2 - 1 \right) \right] + \frac{N_s}{4E_p} X^2. \end{aligned} \quad (10)$$

It is evident that the change in the electronic spectrum due to the presence of the lattice deformation X may be discussed in terms of an effective external field $\tilde{I} \equiv I + X$, so that letting $\tilde{\Delta}_\sigma = \tilde{I} - (\Lambda_c + \sigma \Lambda_s)$, the quasiparticle bands are $E_{k\sigma}^\pm = U/2 \pm \sqrt{\tilde{\Delta}_\sigma^2 + 4\tilde{t}_\sigma^2 \cos^2 k}$. Self-consistency may then be trivially obtained from the results at $g_a=0$, given in Sec. III A. Indeed, the additional self-consistency condition to fix the parameter X simply gives $X = 2E_p m_e$, i.e.,

$$m_e = (2\tilde{I} - 2I)/4t\varepsilon_p. \quad (11)$$

Thus m_e is a linear function of the ratio \tilde{I}/t , for given $I/t, \varepsilon_p$. On the other hand, the solution of the self-consistency equations (8) yields a function $m_e(2\tilde{I}/t)$ of the external field \tilde{I} assumed as given (see Fig. 3). Full self-consistency is obtained as the intersection of this curve and the straight line, Eq. (11), for given values of $2I/t$ and ε_p , yielding the self-consistent values of m_e and \tilde{I} , from which $X = \tilde{I} - I$ is finally determined.

At $I=0, U=0$, the slope of the curve $m_e(2\tilde{I}/t)$ is infinite and a CDW state develops as soon as $\varepsilon_p > 0$, due to the perfect nesting of the Fermi surface. This is the so-called Peierls instability. At $I=0, U>0$, however, the slope of the curve $m_e(2\tilde{I}/t)$ is finite and a finite ε_p is needed to produce a charge modulation with a CDW amplitude that increases with increasing ε_p (see Fig. 6), whereas a phase with coexisting SDW amplitude and lattice deformation does not exist at small ε_p and is a maximum of the free energy, with m_e decreasing with increasing ε_p , for large ε_p .

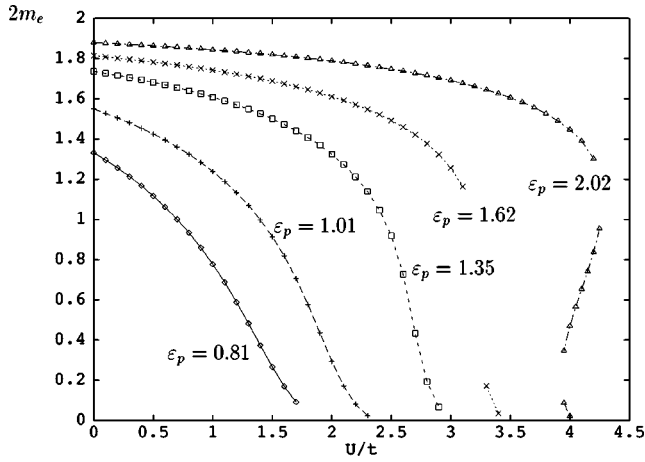


FIG. 6. Charge-density-wave amplitude within the SB approximation as a function of U/t for different values of ε_p . The exponential tails close to the critical points (Ref. 11) are not shown.

Even neglecting the possibility for spin ordering, the CDW phase eventually undergoes a phase transition towards a state without deformation as U/t is increased.¹¹ If ε_p is large enough, this transition becomes of first order. To obtain the phase diagram, it is important to observe that in the undeformed phase ($X=0$) at $I/t=0$ the model reduces to the pure Hubbard model at half-filling. For this latter it is well known that, within the SB approach, the antiferromagnetic phase always has a lower energy than the PM phase.⁸ Since a phase with both lattice deformation and antiferromagnetic structure is not possible at $I=0$, the two competing phases are the CDW and the undeformed SDW.⁴ The transition is always of first order, the two phases having a different symmetry, and is located at $\varepsilon_p \approx U/t$. The resulting phase diagram is given in Fig. 7.

When $I>0$, the possibility for a deformed SDW state arises. Indeed, the straight line, Eq. (11), meets the curves $m_e(2\tilde{I}/t)$ at finite \tilde{I} and m_e (see Fig. 3). When $U/t \geq 2I/t$, the SDW phase has a lower energy than the CDW phase at $\varepsilon_p=0$ (see Sec. III A and Fig. 2). At small ε_p the self-

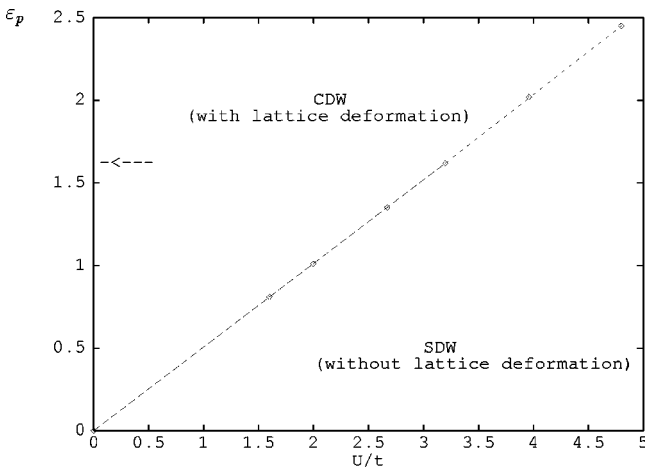


FIG. 7. Phase diagram of the Hubbard model in the presence of a coupling of the local electronic density fluctuations to a lattice deformation within the SB approximation. The arrow indicates the critical value of ε_p beyond which an instability develops within the CDW phase (see text).

consistent solution is very close to the solution at $\varepsilon_p=0$, the straight line, Eq. (11), being almost vertical. However, as ε_p is increased, the CDW amplitude increases much more efficiently in the CDW phase, which is thus more and more competitive with the deformed SDW phase. At a certain critical value for ε_p , a first-order phase transition takes place and at larger ε_p the ground state of the system is PM. Immediately above the phase-transition point, the deformed SDW is still a local minimum of the free energy, but at large enough ε_p a self-consistent solution with coexisting lattice deformation (and related charge modulation) and SDW is no longer possible.

Finally, at $U/t=0$ a CDW phase exists at all $I/t>0$ which is accompanied by a lattice deformation when $\varepsilon_p>0$.

D. The neutral-ionic transition in mixed-stack systems

In this section we want to discuss in more detail the relevance of the results discussed in Secs. III A and III B for a class of organic mixed-stack donor-acceptor crystals, which may be schematically described as a lattice of alternating donor and acceptor atoms, each having two possible configurations. The acceptor may be found either in the neutral configuration (of total charge $Q=0$) or in the singly ionized configuration (of total charge $Q=-1$) with one electron in the lowest unoccupied atomic level of the neutral configuration. The energy difference between the two atomic configurations, taken with a conventional minus sign, is the electron affinity $-E_A$ of the acceptor. The donor is found either in the neutral configuration (of total charge $Q=0$), which we describe as the presence of two electrons of opposite spin in the highest occupied atomic level of the valence multiplet (the core having a charge $Q_{\text{core}}=+2$), or in the singly ionized configuration (of total charge $Q=+1$) when one single electron is left in the highest occupied atomic level. The energy difference between the two atomic configurations, is the ionization energy E_i . The process of a second ionization is usually unfavorable for both atoms, and is neglected by taking the respective energy scales to be infinitely large.

The above situation may be described by means of our model Hamiltonian, Eq. (1), in the limit $U, I \rightarrow \infty$, while the difference $2I-U$ stays finite. In such a limiting case the acceptor sites correspond to the A sites (with local potential $+I$) and the donor sites correspond to the B sites (with local potential $-I$) of the lattice. In the neutral configuration, the atomic energy per site is $(U-2I)/2$, since the B site is doubly occupied and the A site is empty. In the ionized configuration the atomic energy per site is $(I-I)/2=0$ since both the A and the B sites are singly occupied. All other configurations are projected away in the limit considered here. The parameter $\Delta_0=I-U/2$ measures the energy involved in the charge transfer of one electron from the donor to the acceptor and is relevant in the discussion of the resulting phase diagram. We initially neglect the possibility for AFM spin order.

In Fig. 8 we plot the number of electrons on the acceptor site n_a as a function of $\Delta_0/2t$ for different values of the ratio U/t , in the absence of bond dimerization ($\lambda=0$). The ionic and neutral phases are characterized by $n_a>1/2$ and $n_a<1/2$, respectively. At finite U/t there is a continuous crossover from the neutral phase to the ionic phase as $\Delta_0/2t$ is

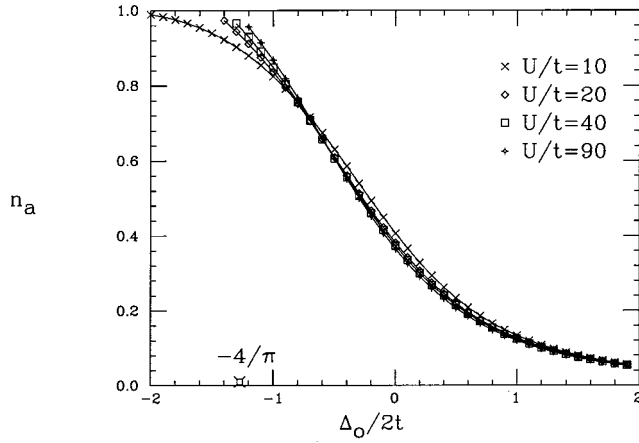


FIG. 8. Density of electrons on the acceptor site, n_a , as a function of $\Delta_0/2t$ for $U/t=10, 20, 40, 90$. The exponential asymptotic behavior was not plotted for $U/t>10$. The transition point in the limit $U/t\rightarrow\infty$ is marked on the horizontal axis. The possibility for AFM spin ordering is neglected here.

decreased. In the limit $U/t\rightarrow\infty$, however, the curve $n_a(\Delta_0/2t)$ becomes nonanalytical at $\Delta_0/2t = -4/\pi$.¹² This point marks the transition to a fully ionized state, with $n_a \equiv 1$ for $\Delta_0/2t \leq -4/\pi$. This transition to a fully ionized phase, which is equivalent to the SB description of the Brinkman-Rice transition in the Hubbard model,^{8,10} might be an artifact of our mean-field approach, and was not found within a real-space renormalization-group approach.¹³ Nonetheless, the quantitative agreement with these results is very good, the acceptor occupancy being very close to unity in the ionic phase.

Within our model, Eq. (1), we may also discuss the effect of a bond dimerization when $\lambda>0$. In Fig. 9 we show that the bond dimerization Y is maximum in the weakly ionized phase, and decreases as $\Delta_0/2t$ is increased, until it vanishes in the neutral phase, which is characterized by the absence of bond dimerization.¹⁴ The behavior of n_a as a function of $\Delta_0/2t$ for different values of λ is shown in Fig. 10. However, if the possibility for a SDW solution is considered, a first ordered phase transition takes place between a dimerized weakly ionized PM phase and an undimerized AFM phase as $\Delta_0/2t$ is reduced. The transition point, according to the phase diagram in Fig. 5, is located at $\Delta_0/2t \approx -0.5$ for large U/t and $\lambda=0$, and is shifted to lower $\Delta_0/2t$ at finite λ (see the inset in Fig. 9). At the transition point the bond dimerization Y jumps discontinuously to zero. However, the ionic PM phase is still a local minimum of the energy, in the region where the AFM phase has a lower energy, and hysteresis phenomena are possible. The acceptor occupancy n_a is larger in the AFM phase at the transition point. The corresponding jump is marked in Fig. 10.

We point out that in our model, Eq. (1), we neglected the effect of the Coulombic interaction in the ionized configuration. If a term

$$-V \sum_I \sum_{\sigma\sigma'} \tilde{f}_{l,\sigma}^+ \tilde{f}_{l,\sigma'} \tilde{f}_{l+1,\sigma'}^+ \tilde{f}_{l+1,\sigma}^-$$

is added to Eq. (1), the Hartree contribution changes I to $I_{\text{eff}} \equiv I + V(n_d - n_a)$, where n_d is the number of electrons on

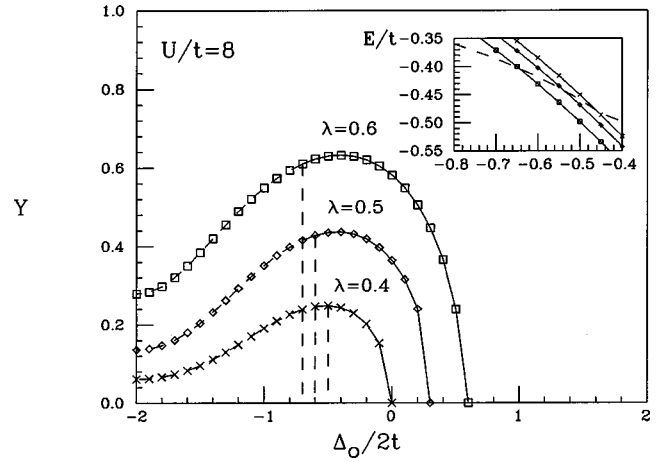


FIG. 9. Bond dimerization Y as a function of $\Delta_0/2t$ for the typical value $U/t=8$ and dimensionless electron-lattice coupling constant $\lambda=0.4, 0.5, 0.6$. The neutral phase at large $\Delta_0/2t$ is always undimerized. The vertical dashed lines locate the first-order transition points towards an undimerized SDW AFM phase, representing the corresponding jumps in the bond dimerization. The Y curves in the metastable PM phase are represented by dashed lines. In this region the AFM phase with $Y=0$ has a lower energy. In the inset, the intersection of the energies in the dimerized PM phase, at the various λ (solid lines, same symbols as in the main figure), with the energy in the undimerized SDW AFM phase (dashed line, independent of λ) locate the first-order phase-transition points.

the donor site. This has the effect of shifting the neutral-ionic transition to larger values of $\Delta_0/2t$, with a sizeable jump of n_a at the transition point. Furthermore, a sizeable nearest-neighbor Coulombic interaction term should prevent the *spurious* appearance of an AFM order¹⁵ within the ionized phase. The detailed analysis of these effects is beyond the scope of this paper and will be reported elsewhere.¹² We limit ourselves to remark that our results are in good quantitative agreement with previous real-space renormalization-group results.¹²

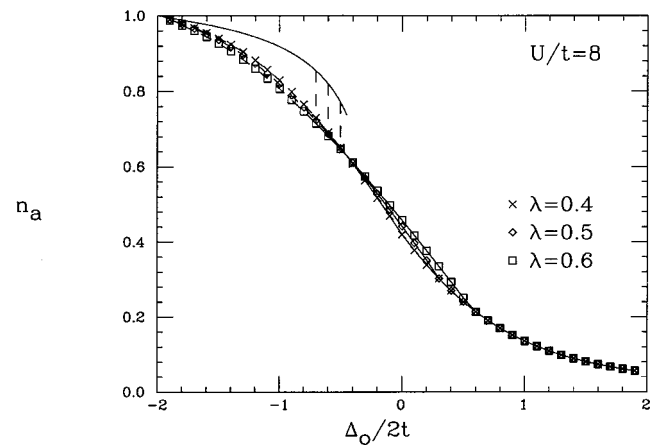


FIG. 10. Density of electrons on the acceptor site, n_a , as a function of $\Delta_0/2t$ for the typical value $U/t=8$ and dimensionless electron-lattice coupling constant $\lambda=0.4, 0.5, 0.6$. The curves collapse in the undimerized neutral phase at large $\Delta_0/2t$. The topmost solid line (independent of λ) represents the acceptor occupancy in the undimerized SDW AFM phase. The dashed vertical lines locate the first-order phase-transition points (see Fig. 9), representing the corresponding jumps in the acceptor occupancy.

IV. CONCLUSIONS

We investigated the competition of spin ordering and dimerization by means of a generalized Hubbard model, both in the case when dimerization is associated with the appearance of a charge modulation and when the dimerization is produced by a deformation of the bonds. We found that when the dimerization is produced by an elastic deformation, it is incompatible with spin ordering, i.e., the system is either dimerized or antiferromagnetic. When the dimerization is imposed by some external field (provided, for instance, by a modulation of the chemical environment of the system), a coexistence of spin order and dimerization becomes possible. As the strength of the intra-atomic potential responsible for spin ordering is reduced, the SDW phase undergoes a first-order phase transition towards a PM dimerized phase, characterized by the presence of a CDW amplitude and/or a bond dimerization.

We also applied our model to describe, in a suitable limiting case, the neutral-ionic transition occurring in mixed-stack donor-acceptor crystals. We found that the ionic phase is characterized by a lattice dimerization when the hopping term is coupled to an elastic lattice deformation, whereas the neutral phase is not dimerized. A first-order phase transition between a PM dimerized ionic phase and an AFM undimerized ionic phase is driven by the increasing influence of the on-site Hubbard term, in the absence of nearest-neighbor and long-range Coulomb interactions.

The limitations of our approach have been discussed in the previous sections. Unfortunately we are not aware of any numerical result which specifically addresses the issue of the competition of charge and spin ordering in dimerized systems including the response of the lattice. This is partly due to the difficulty in extracting the wave amplitudes m_s, m_e in

all known numerical techniques, and in studying realistic (i.e., anisotropic, but not genuinely one-dimensional) systems. Moreover, in a series of recent papers¹⁶ some authors considered models for ferroelectric perovskites and related materials, which are apparently close to our model (1), but they neglected the effect of a self-consistent response of the lattice, so that the resulting phase diagrams cannot be directly compared to ours in any relevant limiting case. Therefore, only a few, well established, results of ours can be tested against numerical results, none of them concerning the competition of charge and spin ordering in dimerized models at issue in the present paper.

As far as the experimental situation is concerned,¹⁷ we point out that our results excludes the possibility of charge and spin ordering in dimerized systems, unless a chemical dimerization forces a charge-modulated state in the system. Thus, most of the low-dimensional nesting-type (or Peierls) CDW systems, such as the molybdenum purple bronzes $\text{KMo}_6\text{O}_{17}$ and $\text{NaMo}_6\text{O}_{17}$, will not support a SDW. On the other hand, systems such as $2H\text{-TaSe}_2$ or $2H\text{-TaS}_2$ seem definitely non-Peierls CDW, so that other mechanisms for CDW formation must be involved. In $1T\text{-TaS}_2$, a strong interplay between charge ordering and on-site correlation has been detected. Systems like this might be candidates for the coexistence of SDW and CDW, since the correlation-driven (Mott-Hubbard) metal-insulator transition takes place within a fully developed CDW state.

ACKNOWLEDGMENTS

S.C. acknowledges partial financial support of the Istituto Nazionale per la Fisica della Materia — Progetto di Ricerca Avanzata 1996.

¹M. Lannoo and G. Allan, *Solid State Commun.* **47**, 153 (1983).
²J.B. Torrence *et al.*, *Phys. Rev. Lett.* **46**, 253 (1981); **47**, 1747 (1981).
³S. Caprara, M. Avignon, and O. Navarro, in *Current Problems in Condensed Matter: Theory and Experiment*, edited by J. L. Moran-Lopez (Plenum, New York, 1998).
⁴J. Bausells and F. Ynduráin, *J. Phys. C* **17**, 5539 (1984).
⁵A similar model, where, however, the direct effect of U on the charge-density-wave amplitude was prevented by subtracting the Hartree contribution in the U term, was studied in V. Tugushev, S. Caprara, and M. Avignon, *Phys. Rev. B* **54**, 5466 (1996).
⁶H. Hasegawa, *J. Phys.: Condens. Matter* **1**, 9325 (1989); *Phys. Rev. B* **41**, 9168 (1990).
⁷S.E. Barnes, *J. Phys. F* **6**, 1375 (1976); P. Coleman, *Phys. Rev. B* **29**, 3035 (1984).
⁸G. Kotliar and A.R. Ruckenstein, *Phys. Rev. Lett.* **57**, 1362 (1986); we refer to this paper for any detail about the SB technique on a bipartite lattice.
⁹In the one-dimensional case, the sums over k in the left-hand side of Eq. (8) can be expressed in terms of complete elliptic integrals as $N_s \rightarrow \infty$. We do not make explicit use of this fact in the

paper, and limit ourselves to point out that this allows for a very accurate numerical solution of the self-consistency equations (8).

¹⁰W.F. Brinkman and T.M. Rice, *Phys. Rev. B* **2**, 4302 (1970).
¹¹H. Zheng, D. Feinberg, and M. Avignon, *Phys. Rev. B* **41**, 11 557 (1990).
¹²S. Caprara and M. Avignon (unpublished).
¹³M. Avignon, C.A. Balseiro, C.R. Proetto, and B. Alascio, *Phys. Rev. B* **33**, 205 (1986).
¹⁴B. Horovitz and J. Sólyom, *Phys. Rev. B* **35**, 7081 (1987).
¹⁵S. Caprara, M. Avignon, and D.D. Sarma, *Int. J. Mod. Phys. B* **11**, 2057 (1997).
¹⁶S. Ishihara, T. Egami, and M. Tachiki, *Phys. Rev. B* **49**, 8944 (1994); S. Ishihara, M. Tachiki, and T. Egami, *ibid.* **49**, 16 123 (1994); R. Resta and S. Sorella, *Phys. Rev. Lett.* **74**, 4738 (1995); G. Ortiz, P. Ordejón, R.M. Martin, and G. Chiappe, *Phys. Rev. B* **54**, 13 515 (1996); R. Resta and S. Sorella, *Phys. Rev. Lett.* **82**, 370 (1999); M. Fabrizio, A.O. Gogolin, and A.A. Nersisyan, *ibid.* **83**, 2014 (1999).
¹⁷For a recent survey see, e.g., M. Grioni and J. Voit, to appear in *Electron Spectroscopies Applied to Low-dimensional Materials*, edited by H. Stanberg and H. Hughes (Kluwer Academic Publ.).